Intermolecular stabilization in new 2-iminopyridine derivatives complexes of Pd(II) and their reactivity towards alkenes

Manuel A. Escobar [a, b, *], David Moreno da Costa [c], Oleksandra S. Trofymchuk [d], Constantin G. Daniliuc [e], Francisco Gracia [a], Fabiane M. Nachtigall [d], Leonardo S. Santos [d], Rene S. Rojas [c], Alan R. Cabrera [c]

[a] *Departamento de Ingeniería Química y Biotecnología, Facultad de Ciencias Físicas y Matemáticas, Universidad de Chile, Beauchef 850, 8370448, Santiago, Chile*
[b] *Departamento de Ciencias Químicas y Biológicas, Universidad Bernardo O'Higgins, General Gana 1702, 8370854, Santiago, Chile*
[c] *Departamento de Química Inorgánica, Facultad de Química, Pontificia Universidad Católica de Chile, Vicuña Mackenna 4860, 702843, Santiago, Chile*
[d] *Instituto de Innovación Basado en Ciencias, Universidad de Talca, 1 Poniente 1141, 747, Talca, Chile*
[e] *Organisch-Chemisches Institut, Universität Münster, Corrensstrasse 40, 48149, Münster, Germany*

ABSTRACT

Two new iminopyriridine ligands (**1**–**2**) and two new neutral Pd(II) complexes (**4**–**5**) were designed, synthesized and characterized by spectroscopic and spectrometric techniques. Molecular structures of compounds **1**, **3** and **5** were obtained by X-Ray Diffraction. Addition of $AgPF_6$ to compounds **4**–**5** produced two new cationic Pd(II) complexes stabilized by an exocyclic nitrile intermolecular interaction (**6**–**7**). The spectrometric characterization of these compounds confirms a dimeric nature of the complexes and an enhanced air/thermal/light resistance. The reactivity towards ethylene oligomerization/polymerization of all complexes (**4**–**7**) at 1 bar was evaluated, either as single component or with 1 equivalent of $B(C_6F_5)_3$. The change of the counterion from PF_6^- to OTf^- allowed to obtain the compound **8**, where an improvement of the reactivity was observed. ESI-MS experiments of **8** showed the insertion of up to 16 units of ethylene in the chain.

© 2018 Elsevier B.V. All rights reserved.

1. Introduction

Polyolefins is one of the most important classes of polymeric materials, which constitutes an important part of the worldwide plastics production [1]. But despite the huge scale of annual production and the wide range of diversity for many applications of these materials, the chain branching control of the polymer is a challenge for the chemists on the development of new methods to ensure materials with best properties [2,3]. To this, homogeneous catalysis based on early-metal catalysts were widely investigated [4—6]. The modulation of their coordination environment allow to develop single-site catalysis that are able to control the key features of the synthesized polymers, such as the mode of main chain linkages, the molecular weight, molecular weight distribution, the

nature of the end-groups, the co-monomer incorporation, sequence along the chain, the linear or branching structure, and the polymer stereochemistry [7—9].

In regard of the ligand environment, the *N,N* α-diimine ligands had been employed in metal complexes for catalysis for many decades. Brookhart et al., reported Ni(II) and Pd(II) catalysts based on bidentate diimine with highly activity in olefin polymerization leading to produce from branched to hyperbranched polyolefins [10—12]. After this discovery, numerous efforts have been focused to develop new catalytic systems using late-transition metals, to obtain polyolefins in high yield, major control in branching and polymer weight [13—16], and thermal-stable catalyst [17—19].

Iminopyridines are versatile bidentate *N,N* ligands that can be easily prepared by condensation of the appropriate pyridine carbonyl compound with an aliphatic or aromatic amine [20—22]. The post-functionalization is usually performed by cross-coupling reactions [23,24] at the heteroaromatic ring. Recently, Chen and col. have developed α-diimine-based nickel and palladium complexes that exhibit a second-coordination- sphere strategy to

influences the properties of the generated catalysts. Here, the ligand interaction is stronger than a halogen, but weaker than ethylene, being able to polymerize and to modulate the characteristic chain-walking feature [2,25].

In this work we report a easily obtained N,N-ligands analogues of (E)-4-(6-((phenylimino)methyl)pyridin-2-yl)benzonitrile (1–2) and the Pd(II) complexes 4–7. These complexes were design with an exocyclic nitrile in the ligand that will allow us to evaluate the effect of this as an intermolecular stabilizing group and possible point of interaction of Lewis acid added to the system. The reactivity of these palladium complexes towards ethylene and 1-hexene was evaluated, as single component or with 1 eq of $B(C_6F_5)_3$ as co-catalyst. These reactions were followed by NMR and ESI techniques [26,27]. In addition, the effect of two counterions in ethylene activation was evaluated.

2. Experimental section

2.1. General

All reagents were purchased from commercial sources, unless otherwise specified. Ligands 3 was prepared as described in literature [28]. Toluene and pentane were distilled from benzophenone ketyl, CH_2Cl_2 was distilled under nitrogen over calcium hydride and chlorobenzene was dried over 4 Å molecular sieves, fractionally distilled under reduced pressure, and stored under a nitrogen atmosphere. The NMR spectra were recorded on NMR Bruker AV 400. Chemical shifts were given in parts per million relative to TMS [^{1}H and ^{13}C, δ(SiMe$_4$) = 0]. Most NMR assignments were supported by additional 2D experiments. HRMS-ESI-MS experiments were carried out using a Thermo Scientific Exactive Plus Orbitrap Spectrometer. FT-IR spectra were recorded on a Bruker Vector-22 Spectrophotometer using KBr pellets. For X-ray crystal structure analysis, data were collected with a D8 Venture Dual Source 100 CMOS diffractometer and with a Bruker APEX II CCD diffractometer by Dr. Constantin G. Daniliuc; full details can be found in the independently deposited crystallography information files (cif). The purity of the compounds was determined by NMR and high resolution mass spectrometry (HRMS).

2.2. Synthesis and characterization

2.2.1. General synthetic procedure of ligands 1–2

4-(6-formylpyridin-2-yl) benzonitrile (1 eq) in anhydrous ethanol (20 mL) was added to a solution of the corresponding aniline (1 eq) and formic acid (catalytic amount) in anhydrous ethanol (20 mL). The mixture was stirred for 12 h at room temperature to give a yellow solution. This solution was filtered and evaporated under vacuum to dryness. The crude product was disolved in CH_2Cl_2 and the solution was washed with water two times. The organic layer was dried over $MgSO_4$. Crude product was purified by recrystallization with hexane. For additional experimental details, 2D NMR and assignments data, see *Supplementary data*.

2.2.1.1. Ligand 1.
Isolated as a yellow solid in 55% yield (0.25 g, 0.90 mmol). ^{1}H NMR (400 MHz, CDCl$_3$, 298 K): δ/ppm = 8.60 (s, 1H, H1), 8.17 (d, J = 7.7 Hz, 1H, H3), 8.10 (d, J = 8.1 Hz, 2H, H9), 7.84 (t, J = 7.8 Hz, 1H, H4), 7.75 (d, J = 7.1 Hz, 1H, H5), 7.69 (d, J = 8.4 Hz, 2H, H8), 7.34 (t, J = 7.6 Hz, 2H, m-Ph), 7.22 (d, J = 6.8 Hz, 2H, o-Ph), 7.20 (t, 1H, p-Ph). ^{13}C{^{1}H} NMR (100 MHz, CDCl$_3$, 298 K): δ/ppm = 160.8 (C1), 155.1 (C7), 155.0 (C2), 150.8 (Ci), 142.9 (C6), 137.7 (C4), 132.6 (C8), 129.3 (Co), 127.5 (C9), 126.9 (Cp), 122.1 (C5), 121.1 (C3), 121.0 (Cm), 118.7 (C10), 112.7 (C≡N). FT-IR (KBr): ν/cm^{-1} = 2228 (C≡N). HRMS(ESI): (C$_{19}$H$_{14}$N$_3$ [M + H$^+$]$^+$): Calc: 284.1188; Found: 284.1175.

2.2.1.2. Ligand 2.
Isolated as a yellow solid in 60% yield (0.45 g, 1.44 mmol) ^{1}H NMR (400 MHz, CDCl$_3$, 298 K): δ/ppm = 8.41 (s, 1H, H1), 8.33 (d, J = 7.7 Hz, 1H, H5), 8.20 (d, J = 8.2 Hz, 2H, H9), 7.97 (t, J = 7.8 Hz, 1H, H4), 7.88 (d, J = 7.8 Hz, 1H, H3), 7.79 (d, J = 8.2 Hz, 2H, H8), 7.10 (d, J = 7.5 Hz, 2H, m-Ph), 6.99 (t, J = 7.4 Hz, 1H, p-Ph), 2.18 (s, 6H, CH$_3$). ^{13}C{^{1}H} NMR (100 MHz, CDCl$_3$, 298 K): δ/ppm = 163.7 (C1), 155.1 (C2), 155.0 (C7), 150.4 (Ci), 143.0 (C10), 137.9 (C4), 132.7 (C8), 128.3 (Cm), 127.7 (C9), 126.9 (Co), 124.3 (Cp), 122.5 (C3), 120.6 (C5), 118.9 (C6), 112.9 (C≡N), 18.4 (CH$_3$). FT-IR (KBr): ν/cm^{-1} = 2227 (C≡N). HRMS(ESI): (C$_{21}$H$_{18}$N$_3$ [M + H$^+$]$^+$): Calc: 312.1501; Found: 312.1487.

2.2.2. General synthetic procedure of complexes 4 and 5

The corresponding ligand (1–3) (1 eq) and [(COD)PdMeCl] (1 eq) were added to a Schlenk flask inside a glovebox. Outside the glovebox, anhydrous and degassed CH_2Cl_2 was added to the mixture (40 mL). The Schlenk flask was protected from light covering with aluminium foil and the mixture was stirred for 24 h at room temperature. The resulting solution was filtered with celite, concentrated and dried under vacuum. The solid was washed several times with hexane to afford pure crystalline material. For additional experimental details, 2D NMR and assignments data, see *Supplementary data*.

2.2.2.1. Complex 4.
Isolated as yellow crystalline material in 65% yield (114 mg, 0.25 mmol). ^{1}H NMR (400 MHz, CD$_2$Cl$_2$, 298 K): δ/ppm = 8.50 (s, 1H, H1), 8.14 (t, J = 7.8 Hz, 1H, H4), 7.95 (d, J = 8.0 Hz, 2H, H8), 7.87 (d, J = 7.9 Hz, 1H, H5), 7.83 (d, J = 7.5 Hz, 1H, H3), 7.79 (d, J = 7.9 Hz, 2H, H9), 7.18 (s, 3H, m-Ph, p-Ph), 2.32 (s, 6H, CH$_3$), 0.47 (s, 3H, Pd-CH$_3$). ^{13}C{^{1}H} NMR (100 MHz, CD$_2$Cl$_2$, 298 K): δ/ppm = 169.1 (C1), 161.3 (C6),152.8 (C2), 146.4 (Ci), 142.4 (C7), 139.9 (C4), 132.5 (C9), 130.9 (C8), 130.4 (C5), 130.1 (Co), 128.9 (Cm), 124.4 (Cp), 127.0 (C3), 119.3 (C≡N), 113.8 (C10), 18.5 (CH$_3$), 1.7 (Pd-CH$_3$). FT-IR (KBr): ν/cm^{-1} = 2228 (C≡N). HRMS(ESI) for (C$_{23}$H$_{19}$N$_4$Pd [M − CH$_4$ + CH$_3$CN]$^+$): Calc: 457.0645; Found: 457.0630. (C$_{24}$H$_{23}$N$_4$Pd [M + CH$_3$CN]$^+$): Calc: 473.0958; Found: 473.0941.

2.2.2.2. Complex 5.
Isolated as pale yellow powder in 62% yield (122 mg, 0.23 mmol). ^{1}H NMR (400 MHz, CD$_2$Cl$_2$, 298 K): δ/ppm 8.48 (s, 1H, H1), 8.14 (t, J = 7.8 Hz, 1H, H4), 7.93 (d, J = 8.0 Hz, 2H, H8), 7.86 (d, J = 7.9 Hz, 1H, H5), 7.83 (d, J = 7.5 Hz, 1H, H3), 7.78 (d, J = 7.9 Hz, 2H, H9), 7.33 (t, 1H, p-Ph), 7.27 (d, 2H, m-Ph), 3.29 (hept, 2H, CH), 1.32 (d, 3H, CH$_3$), 1.16 (d, 3H, CH$_3$), 0.56 (s, 3H, Pd-CH$_3$). ^{13}C{^{1}H} NMR (100 MHz, CD$_2$Cl$_2$, 298 K): δ/ppm = 168.7 (C1), 161.5 (C6),152.5 (C2), 143.9 (Ci), 142.4 (C7), 140.7 (Co), 139.9 (C4), 132.4 (C9), 130.9 (C8), 130.5 (C5), 128.5 (Cp), 127.1 (C3), 124.2 (Cm), 119.3 (C≡N), 113.8 (C10), 28.5 (CH), 25.3 (CH$_3$), 23.0 (CH$_3$), 3.2 (Pd-CH$_3$). FT-IR (KBr): ν/cm^{-1} = 2226 (C≡N) HRMS(ESI) for (C$_{25}$H$_{24}$N$_3$Pd [M − CH$_4$ - CH$_3$CN]$^+$): Calc: 472.1005; Found: 472.0979. For (C$_{27}$H$_{27}$N$_4$Pd [M − CH$_4$ + CH$_3$CN]$^+$): Calc: 513.1271; Found: 513.1255. (C$_{28}$H$_{31}$N$_4$Pd [M + CH$_3$CN]$^+$): Calc: 529.1584; Found: 529.1571.

2.2.3. General synthetic procedure of complexes 6–8

[L^x-Pd(II)MeCl] (4 or 5) (1 eq) and 1 equivalent of AgPF$_6$ or AgOTf, depending on the case, in CH_2Cl_2 was added to a flamed schlenk flask at 0 °C into a glovebox. Then, outside the glovebox was protected from light covering with aluminium foil. The mixture was stirred for 4 h at room temperature. The resulting solution was filtered with celite, concentrated and dried under vacuum. The solid was washed several times with hexane. For additional experimental details, 2D NMR and assignments data, see *Supplementary data*.

2.2.3.1. Complex 6.
Isolated as crystalline yellow solid in 49% yield

(20 mg, 0.035 mol). ^{1}H NMR (400 MHz, CD$_2$Cl$_2$, 298 K): δ/ppm = 8.74 (s, 1H, H1), 8.37 (t, J = 7.1 Hz, 1H, H4), 8.28 (d, J = 7.3 Hz, 1H, H5), 8.06 (d, J = 7.5 Hz, 2H, H8), 7.98 (d, J = 7.5 Hz, 1H, H3), 7.88 (d, J = 7.4 Hz, 2H, H9), 7.22 (s, 3H, m-Ph, p-Ph), 2.33 (s, 6H, CH$_3$), 0.76 (s, 3H, Pd-CH$_3$). ^{13}C$\{^1$H$\}$ NMR (100 MHz, CD$_2$Cl$_2$, 298 K): δ/ppm = 174.5 (C1), 160.3 (C6), 152.0 (C2), 145.3 (Ci), 144.1 (C7), 141.8 (C4), 133.9 (C9), 131.6 (C5), 131.5 (C8), 130.2 (Co), 129.2 (Cm), 128.6 (Cp), 129.7 (C3), 121.5 (C≡N), 112.0 (C10), 18.6 (CH$_3$), 7.9 (Pd-CH$_3$). FT-IR (KBr): ν/cm^{-1} = 2276 (C≡N). HRMS(ESI): (C$_{23}$H$_{19}$N$_4$Pd [M − CH$_4$ + CH$_3$CN]$^+$): Calc: 457.0645; Found: 457.0622. (C$_{24}$H$_{23}$N$_4$Pd [M + CH$_3$CN]$^+$): Calc: 473.0958; Found: 473.0945.

*2.2.3.2. Complex **7**.* Isolated as crystalline yellow solid in 55% yield (22 mg, 0.034 mol). ^{1}H NMR (400 MHz, CD$_2$Cl$_2$, 298 K): δ/ppm = 8.65 (s, 1H, H1), 8.39 (t, 1H, H4), 8.22 (d, J = 7.2 Hz, 1H, H3), 8.08 (d, J = 7.5 Hz, 2H, H8), 8.00 (d, J = 7.6 Hz, 1H, H5), 7.92 (d, J = 7.3 Hz, 2H, H9), 7.40 (t, J = 7.6 Hz, 1H, p-Ph), 7.32 (d, J = 7.7 Hz, 2H, m-Ph), 3.18 (p, J = 6.8 Hz, 2H, CH), 1.36 (d, J = 6.7 Hz, 3H, CH$_3$), 1.21 (d, J = 6.8 Hz, 3H, CH$_3$), 0.85 (s, 3H, Pd-CH$_3$). ^{13}C$\{^1$H$\}$ NMR (100 MHz, CD$_2$Cl$_2$, 298 K): δ/ppm = 173.3 (C1), 160.7 (C6), 151.5 (C2), 144.0 (Ci), 142.7 (C7), 141.9 (C4), 140.8 (Co), 134.0 (C9), 131.9 (C5), 131.5 (C8), 129.5 (C3), 129.4 (Cp), 129.6 (Cm), 121.1 (C≡N), 112.0 (C10), 28.9 (CH), 25.1 (CH$_3$), 22.9 (CH$_3$), 9.6 (Pd-CH$_3$). FT-IR (KBr): ν/cm^{-1} = 2274 (C≡N). HRMS(ESI): (C$_{25}$H$_{24}$N$_3$Pd [M − CH$_4$ - CH$_3$CN]$^+$): Calc: 472.1005; Found: 472.0978. For (C$_{27}$H$_{27}$N$_4$Pd [M − CH$_4$ + CH$_3$CN]$^+$): Calc: 513.1271; Found: 513.1257. (C$_{28}$H$_{31}$N$_4$Pd [M + CH$_3$CN]$^+$): Calc: 529.1584; Found: 529.1569.

*2.2.3.3. Complex **8**.* Isolated as crystalline yellow solid in 55% yield (22 mg, 0.034 mol). ^{1}H NMR (400 MHz, CD$_2$Cl$_2$, 298 K): δ/ppm = 8.64 (s, 1H, H1), 8.36 (t, J = 7.8 Hz, 1H, H4), 8.21 (d, J = 7.8 Hz, 1H, H5), 8.05 (d, J = 8.3 Hz, 2H, H8), 7.97 (d, J = 7.9 Hz, 1H, H3), 7.87 (d, J = 8.4 Hz, 2H, H9), 7.22 (s, 3H, m-Ph, p-Ph), 2.33 (s, 6H, CH$_3$), 0.76 (s, 3H, Pd-CH$_3$). ^{13}C$\{^1$H$\}$ NMR (100 MHz, CD$_2$Cl$_2$, 298 K): δ/ppm = 174.1 (C1), 160.5 (C6), 151.8 (C2), 145.3 (Ci), 144.1 (C7), 141.8 (C4), 133.9 (C9), 131.6 (C3), 131.5 (C8), 130.2 (Co), 129.6 (C5), 129.2 (Cm), 128.6 (Cp), 121.1 (C≡N), 112.0 (C10), 18.7 (CH$_3$), 8.0 (Pd-CH$_3$). FT-IR (KBr): ν/cm^{-1} = 2272 (C≡N).

2.3. ^{1}H NMR scale studies of ethylene oligomerization and 1-hexene isomerization

1 equiv. of palladium complex **6**, **7** or **8** (when was necessary with 1 equiv. of B(C$_6$F$_5$)$_3$), was dissolved in CD$_2$Cl$_2$ (and added 1-hexene ~ 10 mg) into an NMR tube with J. Young valve inside a glovebox. The tube was brought out from the glovebox and attached to a Schlenk line. The tube was frozen and the nitrogen gas was evacuated under vacuum. Ethylene gas was charged through the Schlenk line, and the J. Young valve was closed. ^{1}H NMR spectra were recorded at the corresponding time.

2.4. Ethylene polymerization analysed by ESI-MS

A mixture of palladium complex **4** (4.3 μmol, 2 mg) and saturated solution of ethylene in anhydrous toluene (15.0 mL) was mixed with AgOTf (21.5 μmol, 0.55 mg) (OTf$^-$: triflate) under ethylene atmosphere using a dual-syringe pump operating at a flow rate of 1–100 mL/min in an effective micromixer that was coupled directly to the ion source of the mass spectrometer, and the solution was fed continuously into the MS. The flow rate could be varied from 2.5 to 100 mL/min. By connecting the microreactor directly to the spray capillary, reaction times from 0.9 to 28 s could be covered. ESI-MS and ESI-MS/MS analyses were conducted in a Bruker Daltonics AmaZon SL ion trap mass spectrometer (Bruker Daltonics, Bremen, Germany). The ESI source and the mass

spectrometer were operated in the positive-ion mode, and the capillary voltage and drying gas temperature set to set to +4.0 kV and 220 °C, respectively, with a scan range of m/z 200−5000. Drying gas flow and nebulizing gas pressure were set to 5.0 L/min and 8.0 psi, respectively. MS/MS experiments were carried out by mass selection of a specific ion in ion-trap, which was then submitted to collision-induced dissociation (CID) with helium (He) in the collision chamber.

3. Results and discussion

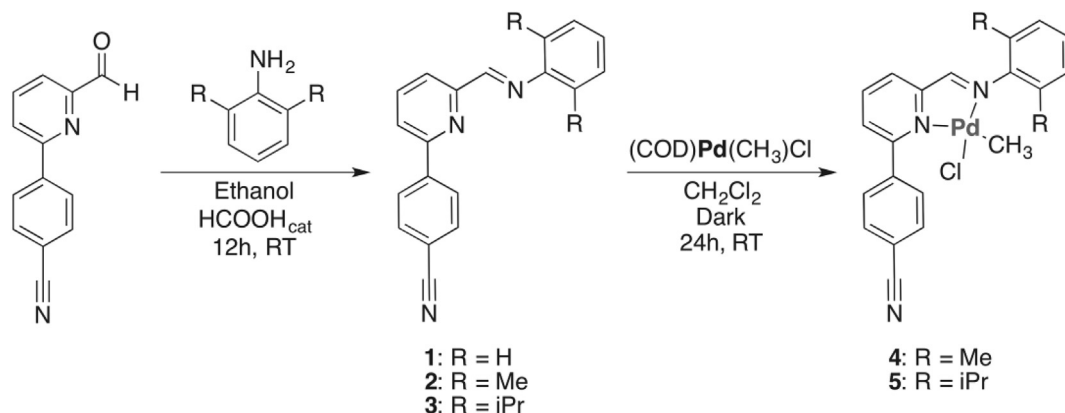### 3.1. Synthesis and characterization of compounds

2-iminopyridine-derived ligands were synthesized following the procedure shown in Scheme 1.4-(6-((phenylimino)methyl)pyridin-2-yl)benzonitrile (**1**) and 4-(6-(((2,6-dimethyl-phenyl)imino)methyl)pyridin-2-yl)benzonitrile (**2**) were synthesized by condensation between4-(6-formylpyridin-2-yl)benzonitrile and the respective 2,6-disubstituted aniline in anhydrous ethanol as solvent according to Scheme 1. Ligand **3** was previously reported [28], however, it's molecular structure is firstly reported in this work. Further recrystallization from hexane gave compounds **1**−**2** in 55% and 60% yield, respectively. Ligands **1**−**2** were completely characterized by ^{1}H and ^{13}C NMR spectroscopy, FT-IR, HRMS and, for ligand **1**, by X-ray crystallography, see Fig. 1 (For characterization of ligands **1**−**2** and the molecular structure of **3** obtained by X-ray diffraction, see *Supplementary data*).

The ligands **1**−**3** have α-diimine core type capable to coordinate the metal centre, and they have alkyl groups at the 2,6-positions of the phenyl ring that introduce the steric hindrance when coordinate to the Pd atom. The 2-position of the ligand pyridine ring possesses a benzonitrile group that allows to modify the electronic effect close to the metal through the coordination of the Lewis acid co-catalysts [29,30]. The molecular structures of ligands **1** and **3** (Fig. 1) show that benzonitrile group is coplanar with respect to the pyridine ring, thus dihedral angle N2-C6-C11-C16 is −14.7(4)° (compound **1**) and N2-C6-C11-C12 is 9.3(2)° (compound **3**). In the case of ligand **1**, the dihedral angle C1-N1-C21-C22 is −167.3(3)°, while for ligand **3** due to the increase of the steric hindrance at the 2,6 positions of the phenyl ring, there is a considerable deviation from the coplanarity, thus the dihedral angle for C1-N1-C21-C26 is −121.5(1)° (For further details see *Supplementary data*).

Treatment of the palladium precursor [(COD)-Pd(CH$_3$)Cl] with **2**−**3** in dichloromethane afforded [(NN)Pd(CH$_3$)Cl] complexes **4**−**5** (see Scheme 1). When ligand **1** was used, the highly insoluble precipitate of respective palladium complex was formed in different solvents (CH$_3$CN, CH$_2$Cl$_2$, THF, Toluene). The obtained palladium complexes **4** and **5** were isolated in 65% and 62% yield, respectively, and were characterized by ^{1}H and ^{13}C spectroscopy, high resolution mass spectrometry, IR and, for compound **5**, X-ray crystallography.

The NMR characterization of the palladium complexes **4** and **5** is consistent with a mononuclear Pd(II) complex with κ^2 ligand coordination mode, and the formation of a single isomer. The determination of the configurational isomer was made through 1D-NOE experiments, where the relative spatial position of the methyl group directly bonded to the Pd atom was study. For complex **4**, it was observed that when the protons of the methyl group were selectively exited (Me-Pd; 0.67 ppm), a NOE effect was observed in the protons of the methyl group of the 2,6-dimethylphenyl substituent (Me; 2.35 ppm). For complex **5**, the proton selectively exited was the −CH unit in the isopropyl group of the 2,6-diisopropylphenyl fragment (^{iPr}CH; 3.34 ppm), observing a NOE effect in the protons of the methyl group directly bonded to the Pd centre (Me-Pd; 0.62 ppm). In both complexes, the experimental

Scheme 1. Synthesis of 2-iminopyridine derivatives **1**–**3** and palladium complexes **4**–**5**.
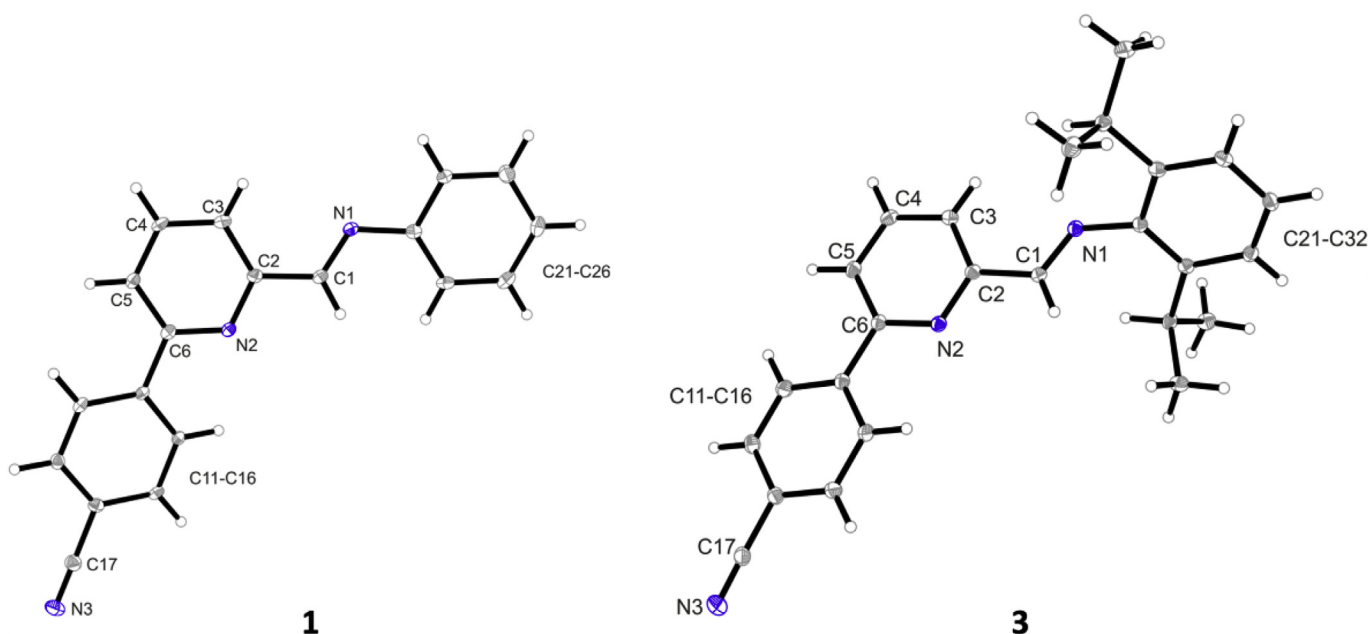

Fig. 1. Molecular structure of ligand **1** (left) and **3** (right). Thermal ellipsoids are shown at the 30% probability level.

NMR data shown that the spatial configuration of the Pd centre is *trans* between the Pd-methyl group and the pyridinic nitrogen atom. On the other hand, the FT-IR spectrum of the complexes exhibited an uncoordinated nitrile group, where the $\nu(CN)$ band does not shift with respect to the free ligand ($\nu \approx 2227$ cm^{-1}).

For complex **5**, its molecular structure was obtained by X-ray diffraction analyses (Fig. 2), in which a square planar geometry at the palladium centre was observed. However, this geometry presents a deviation from planarity due to the repulsion between the *ortho* substituent at pyridine ring and the chlorine atom (dihedral angle for C2-N2-Pd1-Cl1 is 157.8 (3)°). This is consistent with the NMR information obtained, where the Pd centre exhibited a *trans* configurational isomer. On the other hand, 2,6-isopropylphenyl group is orthogonal to the plane of the pyridine ring, with a dihedral angle C1-N1-C21-C22 of −91.4(6)°, being more obtuse with respect to the angle for the free ligand (−121.5(2)°) due to the repulsion with the methyl group attached to the Pd centre. For further details on the spectroscopic and spectrometric characterization of complexes **4** and **5**, see *Supplementary data*.

Has been widely reported that Pd(II) complexes of [(*NN*)PdCH$_3$]$^+$

type can be stabilized through the coordination of an auxiliary ligand to the vacancy of the metal centre [5,31–33]. The most used one is acetonitrile, giving complexes of type [(*NN*)Pd(CH$_3$)*NC*-CH$_3$]$^+$ that have been used as catalysts in oligomerization/polymerization of olefins. Their displacement can be namely by high olefin pressures or by use of Lewis acids co-catalyst as scavengers [34]. In the first case, the displaced auxiliary ligand compete with the olefin for the coordination to the active site, thus decreasing the activity of the catalyst. In the second case, the atom economy is harmed by two aspects: (i) the use of more than one equivalent of Lewis Acid per equivalent of catalyst, and (ii) the formation of a useless acid-base Lewis pair coproduct that does not electronically activate the metal centre. For these reasons, many research groups are looking to either reduce the amount of the Lewis acid co-catalysts used and/ or to improve the remote activation effect.

In response to the above, we set out to explore new options for stabilizing [(*NN*)Pd(CH$_3$)]$^+$ cationic systems without commonly used auxiliary coordinating ligands. Instead, we propose to intermolecularly stabilize the vacancy within two [(*NN*)Pd(CH$_3$)]$^+$ units (Scheme 2). Next, the addition of the Lewis acid to cationic dimers
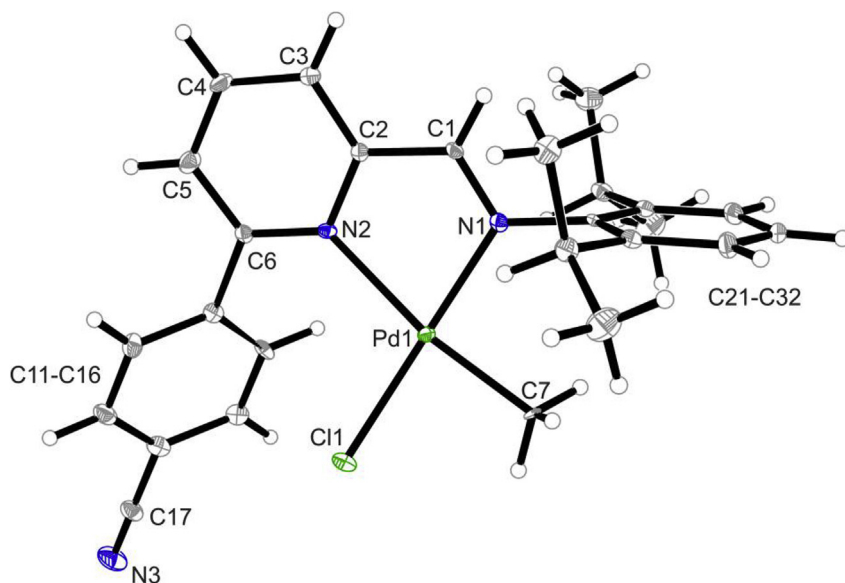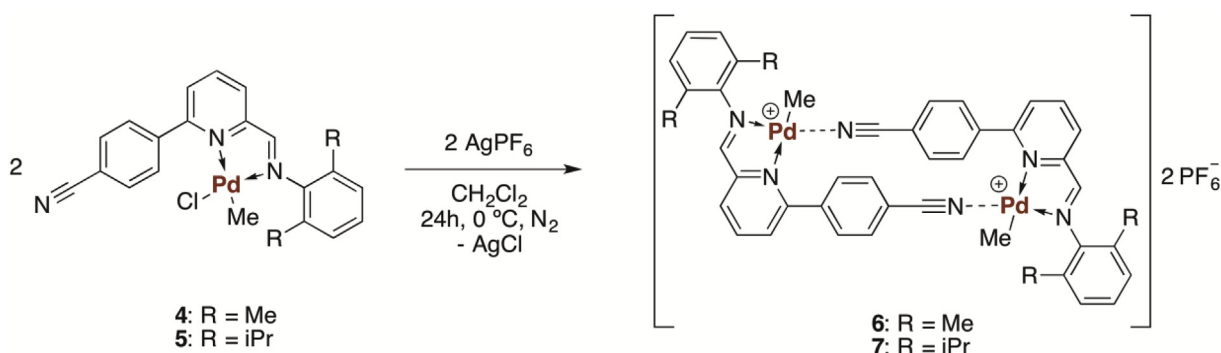
Fig. 2. Molecular structure of palladium complex **5**. Thermal ellipsoids are shown at the 30% probability level.

Scheme 2. Synthesis of intermolecular stabilized dimeric complexes **6** and **7**.

shown on Scheme 2 will allow us to generate the coordinative vacancy *in situ* and by this way to activate the palladium pre-catalyst. In order to achieve this, the chlorine atom of palladium species **4** and **5** was displaced and, once the coordination vacancy on the metal centre was generated, the respective compound was intermolecularly stabilized through the coordination of the nitrile group of another molecule (see compound **6** and **7** on Scheme 2). Thus, cationic palladium dimers **6** and **7** were obtained in 49% and 55% yield, respectively. The ^{1}H NMR characterization of compounds **6** and **7** shown that all chemical shifts undergo a displacement towards low-field. The methyl group bonded to Pd(II) shifts from 0,47 ppm in compound **4** to 0,76 ppm in compound **6**. The iminic proton displaces from 8.50 ppm to 8.74 ppm in compounds **4** and **6**, respectively. This data is consistent with a different chemical species formed by the displacement of the halogen and subsequent coordination of the nitrile. This group prompt a higher removal of electronic density from the metal with a concomitant deshielding of all surrounding atoms. In the same way, the carbon atom of nitrile changes its chemical shift in the ^{13}C NMR from 119.3 ppm (free ligand) to 121.5 and 121.1 ppm for compounds **6** and **7**, respectively. Complexes **6** and **7** presented to be air stable (within 3 days), more photostable than palladium neutral complex and have good solubility in dichloromethane. In order to establish the relative position of the ligand in the dimeric species **6** and **7**, we

performed 1D-NOE experiments in a similar manner than for complexes **4** and **5**. For compound **6** it is observed a NOE effect in the protons of the methyl group of the 2,6-dimethylphenyl sub-stituent (Me; 2.34 ppm) when the protons in the methyl group directly bonded to the palladium atom were selectively irradiated (Me-Pd; 0.77 ppm). For compound **7**, the NOE effect was observed in the protons of the methyl group (Me-Pd; 0.85 ppm) when the proton of the isopropyl group was selectively irradiated (^{iPr}C*H*; 3.17 ppm). These data allow us to infer that the relative configu-ration observed in complexes **4** and **5** it is maintained in the dimeric species **6** and **7**, where the methyl group bonded to Pd(II) is *trans* to the pyridinic nitrogen atom, and therefore, the nitrile group is co-ordinated to the palladium in a *cis* configuration relative to the same nitrogen atom, as can be seen in Scheme 2 (For further compounds characterization see *Supplementary data*).

HRMS analysis of compound **6** with methanol solvent presented a double charged palladium species of *m/z* 432.6 confirming the dimer structure presented on Scheme 2 (For ESI- MS spectra and respective palladium pattern of **6**, see *Supplementary data*). The FT-IR analysis show that ν (CN) band of nitrile group originally located at $\approx$ 2227 cm^{-1} for complexes **4**–**5** was displaced to $\approx$ 2275 cm^{-1}. This displacement of 48 cm^{-1} towards higher energies is consistent with the interaction between the nitrogen lone pair of nitrile group and the Lewis acid (Pd^{+2}) [35–37] (for more details see

Supplementary data).

3.2. Ethylene activation

In order to evaluate the reactivity of the complexes **6** and **7**, ethylene activation experiments were performed at the NMR scale. The reactions were performed under inert atmosphere using an NMR tube with J. Young valve with deuterated dichloromethane as solvent, 1 bar of ethylene and 8 μmol of respective palladium compound. When necessary, 1 equivalent of $B(C_6F_5)_3$ were added to the reaction mixture. The reactions were followed by ^{1}H NMR screening. It should be noted, that complexes **4** and **5** were poorly active toward ethylene, and the use of $AgPF_6$ for activation in dichloromethane leads to complexes **6** and **7**. Finally, we selected the more air/light stable compound **6** for further ethylene activation studies (see discussion below).

The first ethylene activation test was performed with compound **6** as single component catalyst at 25 °C. After 72 h of this reaction ethylene gas was not completely consumed (see Fig. S1). The reaction product was butene with 1:2 distribution between 1-butene and 2-butene, respectively. When the reaction temperature was raised up to 50 °C a considerable increase in ethylene consumption was observed, confirming that compound **6** may act as a single component catalyst. However, after 24 h of the reaction this system was not able to completely consume all ethylene charge, giving 1-butene and 2-butene in a 1:2 ratio (see Fig. S2). Here, despite the low ethylene consumption rate, compound **6** shown a single component catalyst behaviour, where the ethylene displaced the exocyclic nitrile functionality coordinated to the metal centre.

However, we suppose that after the coordination of ethylene, the nitrile group from another molecule of catalyst compete for the coordination vacancy on Pd(II) atom, decreasing the catalytic activity of the respective complex. To avoid this, 1 equivalent of $B(C_6F_5)_3$ was added to complex **6** at 25 °C and ethylene activation test was performed. In this reaction, the ethylene gas was completely consumed after 24 h (see Fig. S3). During the reaction course, the product was changing from 1-butene at the beginning of the reaction to 2-butene at the end of the reaction. Next, the reaction temperature was raised up to 50 °C and under these conditions the system showed the total consumption of ethylene gas during the first hour of reaction. To our delight, under these conditions ethylene was completely consumed even after charging J. Young tube for three times. The reaction product after two charges of ethylene was 2-butene and in the third charging cycle a small fraction of 1-butene was also observed (see Fig. S4). Thus, we confirm that the use of a $B(C_6F_5)_3$ Lewis acid for the activation of dimeric complex **6** allows us to access a faster catalyst activation route. It works as a scavenger of the auxiliary ligand, removing the nitrile functionality attached to palladium and forming an acid-base Lewis pair. Besides, this interaction electronically activates the metal centre by remote activation [29]. The **6** - $B(C_6F_5)_3$ adduct formation, specifically the interaction between the nitrile group and the borane, was followed by ^{13}C NMR. In here, a displacement in the chemical shift corresponding to the $-C{\equiv}N\text{-B}$, from 121.1 ppm in the dimer **6** to 120.0 ppm in the adduct was observed, confirming the acid-base Lewis interaction (see Fig. S15).

In order to explore and clarify the 1-butene isomerization reaction observed, we performed a series of reactions involving a longer α-olefin at NMR scale. The first reaction was the evaluation of the isomerization of 1-hexene by compound **6**, under the same conditions used for ethylene (1 equivalent of $B(C_6F_5)_3$ at 50 °C) and 8 mmol of 1-hexene. It was observed that complex **6** is capable to completely isomerize 1-hexene in 4 h forming only internal hexene isomers, meanwhile olefin insertion products were not observed (see Fig. S8). With this information, we studied the reaction of

complex **6** with ethylene and 1-hexene in the same reaction media, using the conditions tested before. At the beginning of the reaction, when the ethylene concentration is at its maximum, only 1-butene formation is observed (see Fig. S10). However, when the amount of ethylene decreases, the formation of 2-butene as well as the isomerization of 1-hexene was observed, as is depicted in Fig. 3. At this point, both the reinsertion of the eliminated olefin and the insertion of 1-hexene processes compete. As the presence of a larger olefin should not affect the butene isomer distribution in a chain-walking mechanism, we confirm that our compound dimerizes ethylene by a reinsertion/isomerization process of the α-olefin.

On the other hand, we were interested to analyse the effect of the counterion on the reactivity of palladium precatalyst species in ethylene activation reaction and on the type of product that it could generate. For this purpose, 1 equivalent of AgOTf was added to palladium compound **4** in dichloromethane to obtain compound **8**. This compound was characterized by NMR and FT-IR. In addition, 1D NOE experiment was performed to determine the relative position of the ligand around the metal centre. After the selective irradiation of the protons of the methyl group directly bonded to Pd(II) atom (Me-Pd; 0.76 ppm), a NOE effect was observed in the protons of the methyl group of the 2,6-dimethylphenyl substituent (Me; 2.33 ppm). Consequently, these spectroscopic data are in concordance with those from dimers **6** and **7**, where the methyl group (Me-Pd) is in *trans* position to the pyridinic nitrogen atom and the nitrile group of another molecule is in *cis* configuration relative to the same nitrogen (For further compound characterization see *Supplementary data*).

The reactivity towards ethylene of compound **8** was realized under the same conditions that dimer **6** was studied. For this, the catalytically active species was generated *in situ* and once the complex was formed, ethylene was charged into the NMR tube at 1 bar of pressure and the reaction was monitored at 25 °C. After 6 h, the entire charge of ethylene was consumed (see Fig. S12), corroborating that this single component species has a higher reactivity towards the olefin than complex **6**. In addition, the reaction with ethylene was studied using 1 equivalent of $B(C_6F_5)_3$ as co-activator. Surprisingly, the total consumption of ethylene in less than 15 min was observed. Moreover, this adduct was able to made two cycles of ethylene recharge before the decomposition and the consequent inactivation of its occurs. From the point of view of the product obtained, compound **8** mainly shown the formation of 1-butene and 2-butene, and in a lesser extent larger products than those generated with complex **6** (see Fig. S13). Whereas **8**/$B(C_6F_5)_3$ was able to produce only 2-butene. In fact, the removal of the nitrile from the reaction medium by the coordination with a Lewis acid promotes the β-elimination and therefore decreases the quantity of larger olefins products.

The difference in the reactivity of compounds **6** and **8** can be discussed considering the nature of both counterions. Whilst in a first analyses of the triflate anion structure it can be argued that is a more coordinating ion than hexafluorophosphate. It is known that the electron delocalization in some structure result in the stabilization of this and reduce the coordination character against bulky cations, as was argued by Ramesh and Lu for a very similar counter ion [38]. On the contrary, hexafluorophosphate anion does not show any resonance structure. Therefore, the triflate anion can be easily dissociated in comparison to the hexafluorophosphate anion and, consequently, is less coordinating. Besides, the size of triflate ion is bigger than hexafluorophosphate ($OTf^- \approx 87 \text{ Å}^3$ versus $PF_6^- \approx 73 \text{ Å}^3$) [38]. In consequence, OTf^- should be positioned in a second coordination sphere, far beyond the assumed position of the PF_6^-. On account of this, our results are in agreement with a higher "spectator" behaviour of the triflate counterion than the
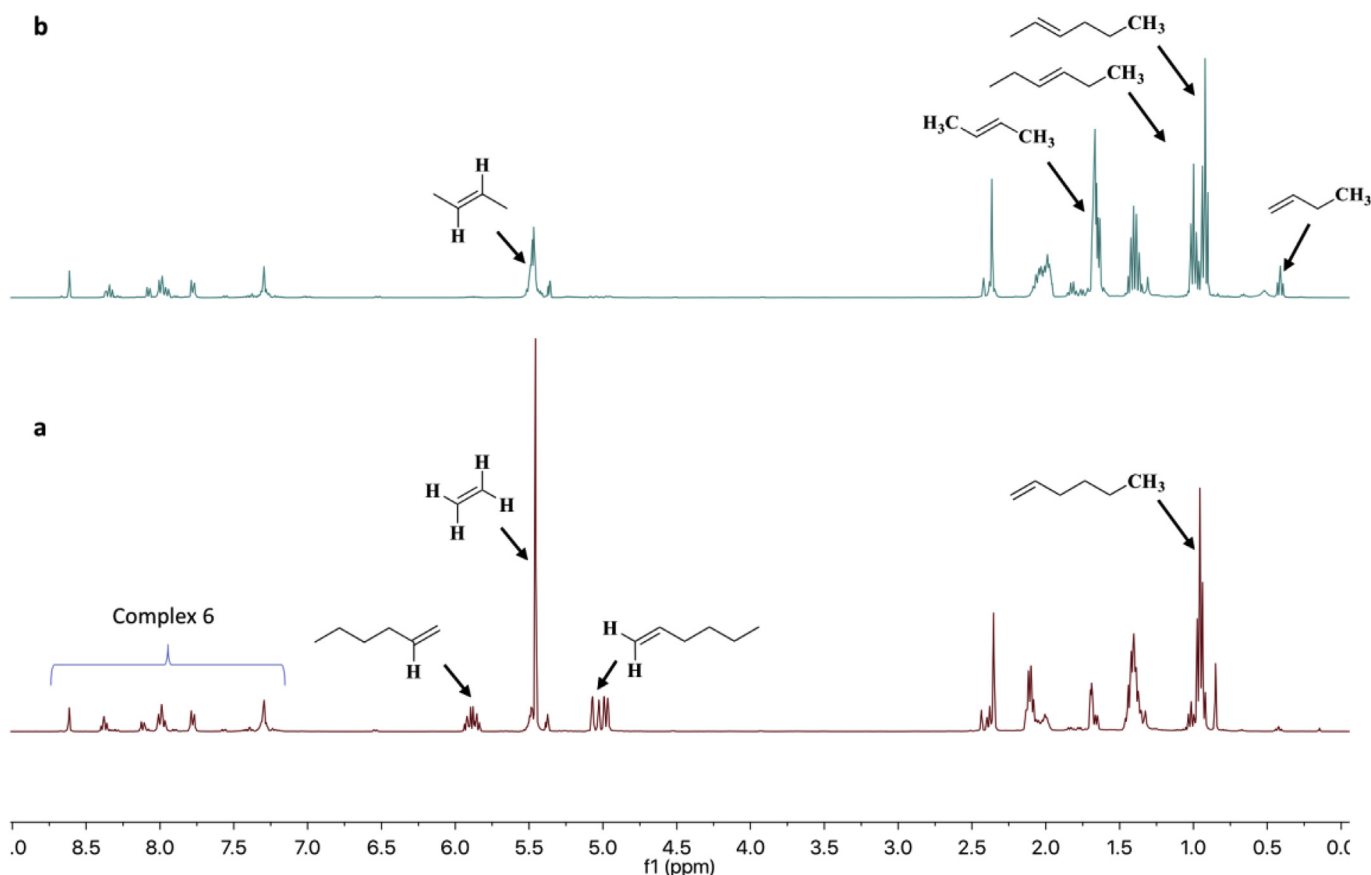
Fig. 3. ^{1}H NMR spectra of ethylene and 1-hexene activation with **6** + 1 eq B(C$_6$F$_5$)$_3$ at 50 °C, a) initial, b) final.

hexafluorophosphate one, as was observed in a higher reactivity of compound **8** than compound **6**.

3.3. Catalyst activation and ethylene polymerization analysed by ESI

In order to elucidate the possible mechanism of ethylene oligomerization/polymerization and identify the active species, we have performed ESI-MS screening of the reaction between **4**/AgOTf and ethylene. For this, a mixture of **4**/ethylene (saturated solution of C$_2$H$_4$ in toluene) was mixed with AgOTf (solution in toluene) in anhydrous toluene using a dual-syringe pump operating at different flow rates in an effective micromixer, that was coupled directly to the ion source of the mass spectrometer, and the solution was fed continuously into the mass spectrometer. During this experiment, differences in the growth of polymer with time were observed. After 12—18 min of the reaction we were able to detect two series of ions, the odd chain, result of the ethylene insertion into palladium (denoted as green on Fig. 4, 11—16 insertions of ethylene, of m/z 740.5—880.5, [**2**-Pd(C$_2$H$_4$)$_n$CH$_3$]$^+$, Fig. 4) and even-chain (denoted as red, [**2**-Pd(C$_2$H$_4$)$_{n-1}$CH$_3$]$^+$, 9—15 insertions of ethylene, of m/z 669.5—866.5), result of the ethylene insertion into palladium hydride species. Moreover, further characterization of several Pd-alkyl ions found in these experiments was achieved through ESI-MS/MS experiments confirming the presence of palladium as judged by the release of [**2**-PdH]$^+$. Finally, we also were able to detect the presence of palladium hydride active species [**2**-PdH]$^+$ of m/z 418.1 directly intercepted from the solution.

The activation pathway of **4** (**a**) is shown on Scheme 3 and starts with the presence of AgOTf, which subtract a chlorine atom

forming a vacancy (see species **b**). Subsequent insertions of molecules of ethylene into **b** result in the formation of compound **c**. After the β-elimination, **c** releases an alkene, a palladium hydride complex is formed (**d**). Next, palladium hydride **d** inserts molecules of ethylene giving rise to palladium-alkyl species **e**, that eliminates alkenes and the active palladium hydride **d** is regenerated.

4. Conclusions

In this work, we have described the successfully synthesis and characterization of new 2-iminopyridine derivatives ligands **1**—**2** with a nitrile exocyclic functionality in their structures. Besides, the synthesis and characterization of new neutral palladium complexes **4**—**5** were also described. These complexes in presences of 1 equivalent of AgPF$_6$ form an air and light stable cationic palladium dimers (**6**—**7**), and with 1 equivalent of AgOTf produces compound **8**.

The reactivity towards ethylene at 1 bar and variable temperature (25 °C and 50 °C) of all complexes were tested. The cationic dimer **6** presented to be the more active complexes among those with PF$_6^-$ towards ethylene, acting as single component catalyst. Nevertheless, by adding 1 equivalent of B(C$_6$F$_5$)$_3$ we obtained a species that was able of consume ethylene at least 20-folds faster than without the co-catalyst. The product in the reactions were mainly 1-butene and/or 2-butene, depending on the conditions used.

The study of the reaction of **6** with 1-hexene, under the same conditions used for ethylene, confirmed that the reinsertion of the eliminated olefin and the insertion of 1-hexene processes compete between each other. This result allows us to suggest that our
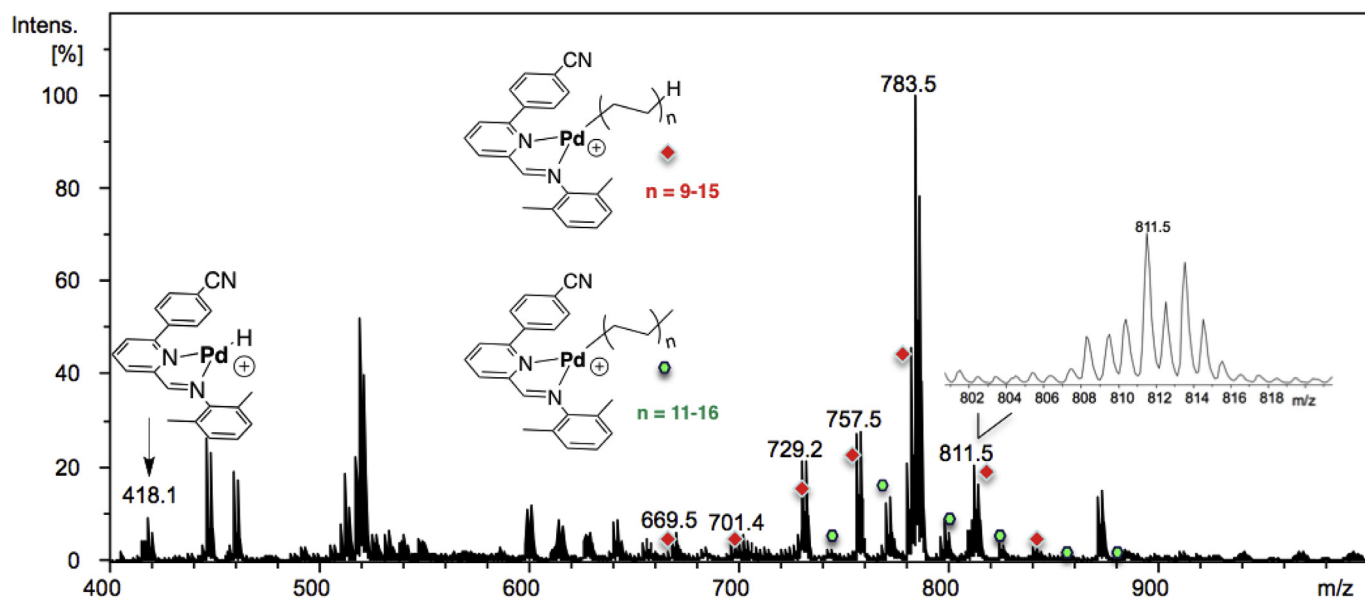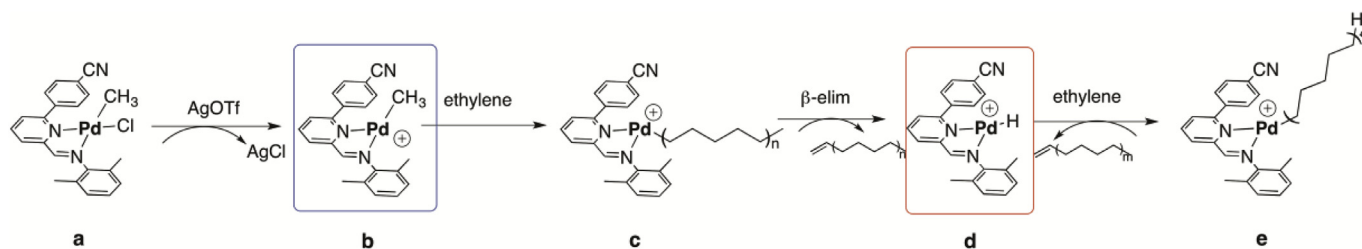
Fig. 4. ESI mass spectrum of a sample from the catalytic reaction. After reaction times of 12–18 min showing higher intensity odd-chain (denoted as green) and even-chain (denoted as red) product series using a microreactor. (For interpretation of the references to colour in this figure legend, the reader is referred to the Web version of this article.)

Scheme 3. Catalytic activation of ethylene with **4**/AgOTf.

compound dimerizes ethylene by a reinsertion/isomerization process of the α-olefin, instead of a chain-walking mechanism.

On the other hand, the effect of the counterion was evaluated by using the compound **8**, which have a triflate anion as a counterion. This new species showed a higher reactivity towards the olefin than complex **6** (PF_6^-), acting as single component with 12-fold faster consumption of ethylene. As well as, the addition of 1 equivalent of $B(C_6F_5)_3$ form a catalytic species able to increases the consumption of ethylene up to 24-fold faster than without the Lewis acid and an impressive 100-fold than with PF_6^- as counterion, under the same conditions. In addition, the ESI-MS experiment of compound **8** shown the formation of larger products than those generated with complex **6** (PF_6^-), with the insertion of up to 16 units of ethylene to the chain.

Finally, we have demonstrated that the use of a methodology where the nitrile groups within the ligand structure stabilize the coordination vacancy of the palladium centre allow us to generate a more active catalyst. Moreover, the use of triflate as counter ion produce a more reactive species, capable of produce larger oligomers of ethylene. These results encourage us to continue our research in Pd(II) complexes activation, intermolecular stabilization, the evaluation of the catalytic activities at high pressures of ethylene and copolymerization with polar monomers.

Appendix B. Supplementary data

Supplementary data related to this article can be found at https://doi.org/10.1016/j.jorganchem.2018.03.032.

References

[1] M. Sturzel, S. Mihan, R. Mulhaupt, Chem. Rev. 116 (2016) 1398–1433.
[2] M. Li, X. Wang, Y. Luo, C. Chen, Angew. Chem. Int. Ed. 56 (2017) 11604–11609.
[3] J.-Y. Dong, Y. Hu, Coord. Chem. Rev. 250 (2006) 47–65.
[4] P. Mountford, Dalton Trans. 42 (2013) 8977–8978.
[5] L.R. Sita, Angew. Chem. Int. Ed. 50 (2011) 6963–6965.
[6] V. Busico, Dalton Trans. (2009) 8794–8802.
[7] G.W. Coates, P.D. Hustad, S. Reinartz, Angew. Chem. Int. Ed. 41 (2002) 2236–2257.
[8] G.W. Coates, J. Chem. Soc., Dalton Trans. (2002) 467–475.
[9] G.J. Domski, J.M. Rose, G.W. Coates, A.D. Bolig, M. Brookhart, Prog. Polym. Sci. 32 (2007) 30–92.
[10] L.K. Johnson, C.M. Killian, M. Brookhart, J. Am. Chem. Soc. 117 (1995) 6414–6415.
[11] S. Mecking, L.K. Johnson, L. Wang, M. Brookhart, J. Am. Chem. Soc. 120 (1998) 888–899.
[12] C.M. Killian, D.J. Tempel, L.K. Johnson, M. Brookhart, J. Am. Chem. Soc. 118 (1996) 11664–11665.
[13] D. Bézier, O. Daugulis, M. Brookhart, Organometallics 36 (2017) 2947–2951.
[14] T. Vaidya, K. Klimovica, A.M. LaPointe, I. Keresztes, E.B. Lobkovsky, O. Daugulis,

G.W. Coates, J. Am. Chem. Soc. 136 (2014) 7213–7216.

[15] D. Takeuchi, Y. Chiba, S. Takano, K. Osakada, Angew. Chem. Int. Ed. 52 (2013) 12536–12540.

[16] D. Liu, C. Yao, R. Wang, M. Wang, Z. Wang, C. Wu, F. Lin, S. Li, X. Wan, D. Cui, Angew. Chem. Int. Ed. 54 (2015) 5205–5209.

[17] H. Hu, L. Zhang, H. Gao, F. Zhu, Q. Wu, Chem. Eur J. 20 (2014) 3225–3233.

[18] S. Kong, K. Song, T. Liang, C.Y. Guo, W.H. Sun, C. Redshaw, Dalton Trans. 42 (2013) 9176–9187.

[19] J. Liu, D. Chen, H. Wu, Z. Xiao, H. Gao, F. Zhu, Q. Wu, Macromolecules 47 (2014) 3325–3331.

[20] A. Boudier, P.-A.R. Breuil, L. Magna, H. Olivier-Bourbigou, P. Braunstein, Chem. Commun. (J. Chem. Soc. Sect. D) 50 (2014) 1398–1407.

[21] L. Zhang, X. Hao, W.-H. Sun, C. Redshaw, ACS Catal. 1 (2011) 1213–1220.

[22] C. Bianchini, G. Giambastiani, L. Luconi, A. Meli, Coord. Chem. Rev. 254 (2010) 431–455.

[23] C. Bianchini, G. Mantovani, A. Meli, F. Migliacci, Organometallics 22 (2003) 2545–2547.

[24] T. Irrgang, S. Keller, H. Maisel, W. Kretschmer, R. Kempe, Eur. J. Inorg. Chem. (2007) 4221–4228.

[25] L. Guo, S. Dai, X. Sui, C. Chen, ACS Catal. 6 (2016) 428–441.

[26] M.A. Escobar, O.S. Trofymchuk, B.E. Rodriguez, C. Lopez-Lira, R. Tapia, C. Daniliuc, H. Berke, F.M. Nachtigall, L.S. Santos, R.S. Rojas, ACS Catal. 5 (2015) 7338–7342.

[27] A.R. Cabrera, I. Martinez, C.G. Daniliuc, G.B. Galland, C.O. Salas, R.S. Rojas, J. Mol. Catal. Chem. 414 (2016) 19–26.

[28] M. Novák, H. Hošnová, L. Dostál, B. Glowacki, K. Jurkschat, A. Lyčka, Z. Ruzickova, R. Jambor, Chem. Eur J. 23 (2017) 3074–3083.

[29] B.M. Boardman, J.M. Valderrama, F. Muñoz, G. Wu, G.C. Bazan, R. Rojas, Organometallics 27 (2008) 1671–1674.

[30] C.B. Shim, Y.H. Kim, B.Y. Lee, Y. Dong, H. Yun, Organometallics 22 (2003) 4272–4280.

[31] G. Canil, V. Rosar, S.D. Marta, S. Bronco, F. Fini, C. Carfagna, J. Durand, B. Milani, ChemCatChem 7 (2015) 2255–2264.

[32] A. Tognon, V. Rosar, N. Demitri, T. Montini, F. Felluga, B. Milani, Inorg. Chim. Acta. 431 (2015) 206–218.

[33] W. Tao, S. Akita, R. Nakano, S. Ito, Y. Hoshimoto, S. Ogoshi, K. Nozaki, Chem. Commun. (J. Chem. Soc. Sect. D) 53 (2017) 2630–2633.

[34] A.L. Kocen, K. Klimovica, M. Brookhart, O. Daugulis, Organometallics 36 (2017) 787–790.

[35] A.R. Cabrera, R.S. Rojas, M. Valderrama, P. Plüss, H. Berke, C.G. Daniliuc, G. Kehr, G. Erker, Dalton Trans. 44 (2015) 19606–19614.

[36] A.R. Cabrera, E. Villaseñor, F. Werlinger, R.S. Rojas, M. Valderrama, A. Antiñolo, F. Carrillo-Hermosilla, R. Férnadez-Galan, J. Mol. Catal. Chem. 391 (2014) 130–138.

[37] K. Spannhoff, R. Rojas, R. Fröhlich, G. Kehr, G. Erker, Organometallics 30 (2011) 2377–2384.

[38] M. Yamada, H. Hagiwara, H. Torigoe, N. Matsumoto, M. Kojima, F. Dahan, J.-P. Tuchagues, N. Re, S. Iijima, Chem. Eur J. 12 (2006) 4536–4549.